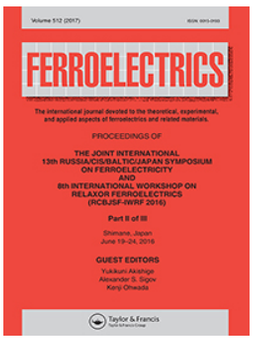

Ferroelectrics

ISSN: 0015-0193 (Print) 1563-5112 (Online) Journal homepage: http://www.tandfonline.com/loi/gfer20

Electrical properties of PMN-33PT thin film at MPB

R. Mackeviciute, R. Grigalaitis, J. Banys, M. Boota, A. Ghosh & G. Rijnders

To cite this article: R. Mackeviciute, R. Grigalaitis, J. Banys, M. Boota, A. Ghosh & G. Rijnders (2017) Electrical properties of PMN-33PT thin film at MPB, Ferroelectrics, 512:1, 1-7, DOI: 10.1080/00150193.2017.1355140

To link to this article: https://doi.org/10.1080/00150193.2017.1355140

FERROELECTRICS
2017, VOL. 512, 1–7
https://doi.org/10.1080/00150193.2017.1355140

Taylor & Francis
Taylor & Francis Group

Electrical properties of PMN-33PT thin film at MPB

R. Mackeviciute[a], R. Grigalaitis[a], J. Banys[a], M. Boota[b], A. Ghosh[b], and G. Rijnders[b]

[a]Vilnius University, Faculty of Physics, Vilnius, Lithuania; [b]University of Twente, Faculty of Science & Technology, Enschede, The Netherlands

ABSTRACT

This paper presents a systematic investigation of the electric properties of epitaxial PMN-33PT thin film as a function of temperature and frequency. Complex impedance measurements were performed over the temperature range of 30 – 500 K and frequency range 20 Hz – 1 MHz. Obtained results were corrected for the SRO series resistance. Ferroelectric hysteresis loops and electric field tunability of the real part of dielectric permittivity were measured in the 300 K – 450 K temperature range and at a frequency of 1 kHz. The results of electrical field tunability of complex dielectric permittivity were approximated by Landau-Ginsburg-Devonshire theory frame by the Johnson relation. Meanwhile, ferroelectric hysteresis loop measurements of epitaxial PMN-33PT thin film shows a good hysteresis property with a remnant polarization of $2P_r \approx 10\ \mu C/cm^2$ and coercive field of $2E_c \approx 12$ kV/cm at temperature range from 300 K to 380 K.

ARTICLE HISTORY
Received 19 June 2016
Accepted 27 March 2017

KEYWORDS
PMN-33PT; electrical properties; MPB

Introduction

Ferroelectric oxides, most notably $PbZr_{1-x}Ti_xO_3$ (PZT), are considered as promising candidates for micro electromechanical systems (MEMS) [1, 2]. An alternative to PZT is a relaxor ferroelectric like $Pb(Mg_{1/3}Nb_{2/3})O_3$-$PbTiO_3$ (PMN-PT), which is a solid solution between a relaxor (PMN) and a ferroelectric (PT) material. In this system, with the increase in the PT content, T_C increases and relaxor behavior decreases and between PMN-30PT to PMN-50PT compositions, there exists a morphotropic phase boundary (MPB) which is associated with abnormally high dielectric response and giant electromechanical properties [3]. The nature of the MPB is still debated in the literature, but a consensus seems to emerge on the existence of a sequence of second order phase transitions that accommodate the rhombohedral to the tetragonal transition, thus allowing for easy rotation of the polarization vector [4]. The MPB phase boundary occurs at 33% PT of the PMN-PT solid solution system [5]. The piezoelectric, pyroelectric and dielectric responses of PMN-PT at MPB are anomalously large [6, 7]. There are several reports presented in the field of electrical properties of PMN-PT thin films. K. Wasa et al. studied properties of sputtered and single c-

CONTACT R. Mackeviciute Ruta.Mackeviciute@ff.vu.lt Vilnius University, Faculty of Physics, Sauletekio av. 9, III b. 817, LT-10222 Vilnius, Lithuania.

Color versions of one or more of the figures in the article can be found online at www.tandfonline.com/gfer.

domain/single crystal PMN-33PT thin films [8–10]. Hence, taking into account the extraordinary properties of PMN-PT at MPB and the fact that for many applications, one requires materials in thin film form, it is very crucial to present systematic electrical properties of epitaxial PMN-PT thin film near the MPB. In this work, we present complex impedance measurements, ferroelectric hysteresis loops and electric field tunability measurements of epitaxial PMN-33PT thin film as function of applied electric field.

Experimental details

Epitaxial $Pb(Mg_{1/3}Nb_{2/3})O_3$-$33PbTiO_3$ (PMN-33PT) thin film of 500 nm thickness was deposited by pulsed laser deposition technique (PLD) using a KrF excimer laser ($\lambda = 248$ nm) on (001) oriented $SrTiO_3$ substrate. $SrRuO_3$ (SRO) was used as base and top electrodes with thickness equal to 100 nm. More detailed deposition conditions of PMN-33PT functional layer and SRO electrodes are reported elsewhere [11,12].

An HP4284 precision LCR-meter was used for complex impedance measurements at temperatures from 500 K to 300 K during the cooling cycle at a rate of about 1 K/min and frequencies ranging from 20 Hz to 1 MHz. Ferroelectric hysteresis loops and electric field tunability of real and imaginary parts of dielectric permittivity were measured in the 300 – 450 K temperature range and at a frequency of 1kHz. Measurements were performed using an aixACCT TF Analyser 3000 ferro- and piezoelectric thin film analysis system.

Results and discussion

The frequency dependencies of the real and imaginary parts of the impedance of the PMN-33PT thin film is shown in Fig. 1. To gain information about processes in the

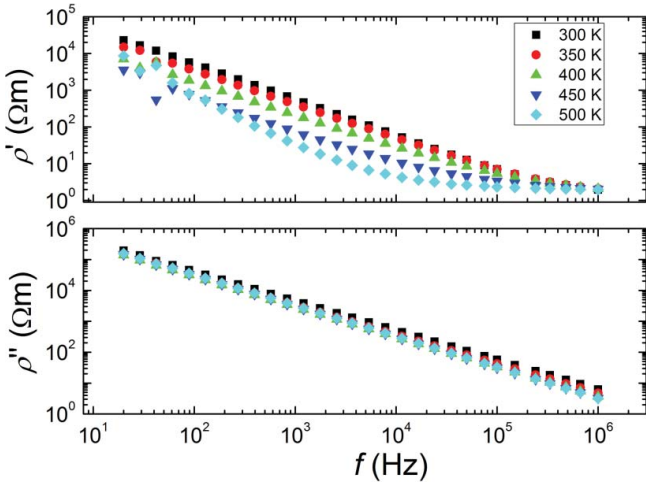

Figure 1. Frequency dependence of the real and imaginary parts of specific impedance.

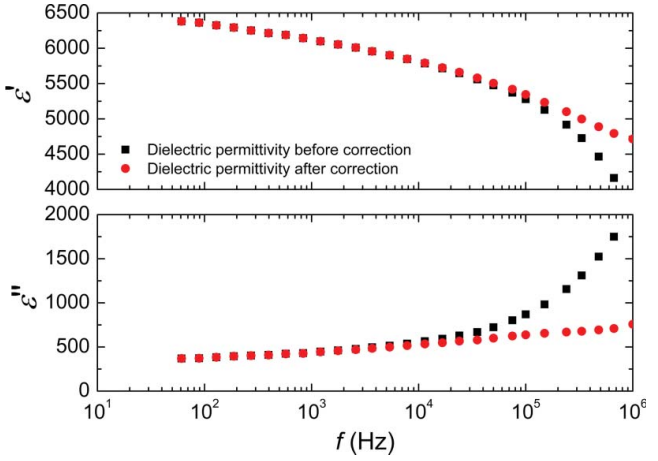

Figure 2. Frequency dependence of the complex dielectric permittivity, before (black squares) and after (red dots) correction for the series resistance due to the electrodes.

PMN-33PT thin film, the complex dielectric permittivity was calculated from these results.

Figure 2 shows the frequency dependences of the real and imaginary part of the complex dielectric permittivity before and after correction for the series resistance due to the SRO electrode, calculated from the measured impedance using Eq. 1.

$$\begin{aligned} \rho'_{\mathrm{cor}} &= \rho'_{\mathrm{exp}} - \rho_{\infty} \\ \rho''_{\mathrm{cor}} &= \rho''_{\mathrm{exp}} \end{aligned} \tag{1}$$

Here ρ'_{cor} and ρ''_{cor} correspond to the real and imaginary parts of the corrected measured resistance, ρ'_{exp} and ρ''_{exp} corresponds to the experimentally results of real and imaginary parts of specific resistance and ρ_{∞} corresponds to serial resistance of SRO electrode.

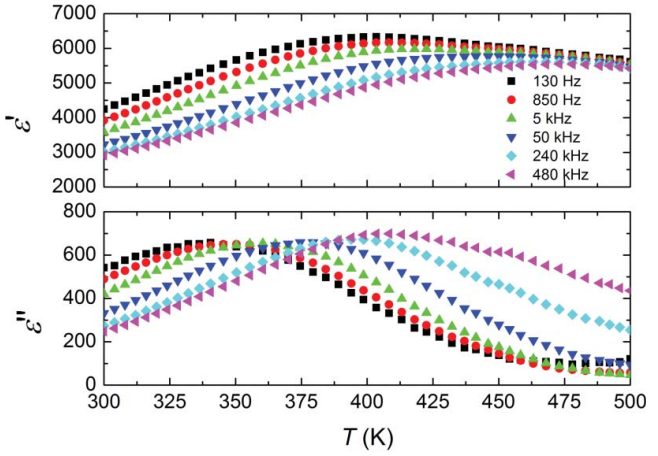

Figure 3. Temperature dependence of complex dielectric permittivity after correction.

Corrections at frequencies from 100 kHz were made by subtracting the constant value of serial resistance of SRO electrode ($\rho_\infty = 2\ \Omega$m). It is obvious from Fig. 2 that after this correction, the change of the complex dielectric permittivity with frequency at high frequencies is strongly reduced.

Dielectric permittivity values recalculated from the complex resistivity, measured as function of temperature and excitation frequency are presented in Fig. 3. The real part of the dielectric permittivity shows two broad and overlapping dielectric anomalies: first one around 400 K and another around 480 K. The dielectric constant of PMN-33PT thin film is approximately equal to 6000.

The electric field tunability of the real part of the dielectric permittivity is presented in Fig. 4a in the temperature range 300 to 450 K. Dots represent the experimental points and lines represent the Johnson approximation of the Landau-Ginsburg-Devonshire (GLD)

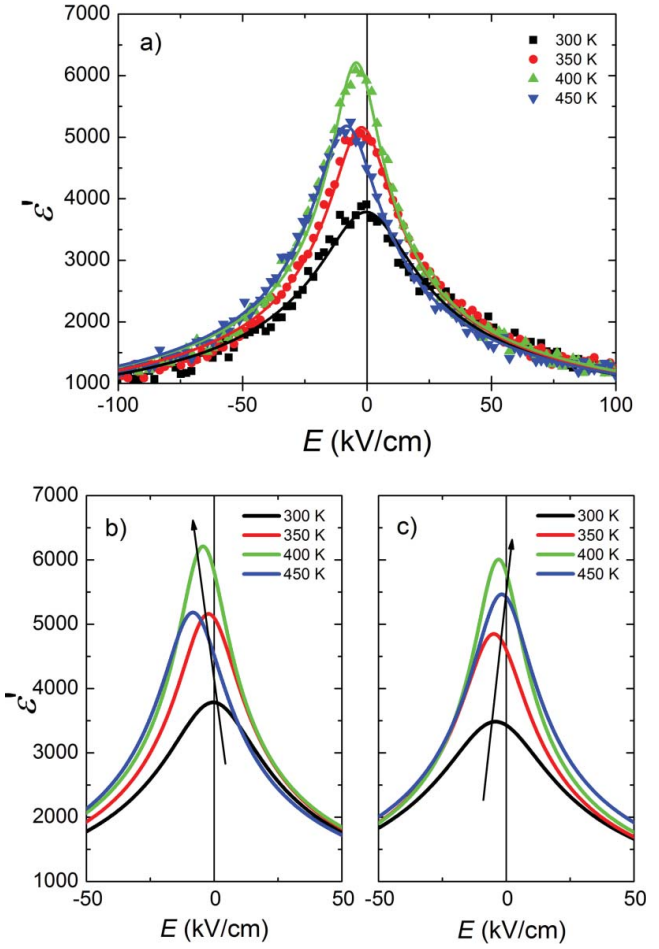

Figure 4. (a) Electric field tunability of the real part of the dielectric permittivity. Dots represent the experimental points and lines represent the Johnson approximation of the Landau-Ginsburg-Devonshire (b) and (c) experimental results approximation when the field is changed from positive to negative and vice versa, respectively.

theory [13], eq. (2).

$$\varepsilon(E) = \frac{\varepsilon(0)}{\left\{1 + 3\beta[\varepsilon_0\varepsilon(0)]^3(E + \Delta E)^2\right\}^{1/3}} \tag{2}$$

Here, E – electric field β – material constant in GLD model, ΔE – displacement from the zero position, ε_0 - dielectric constant of vacuum, $\varepsilon(0)$ – the maximum value of dielectric permittivity.

Figure 4b and 4c represent the measured and fitted curves when the field is changed from positive to negative and vice versa, respectively (see Eq. 2). It is clearly seen that the position of the maximum of dielectric permittivity strongly depends on the direction of the applied electric field. This might be due to charge injection from bottom electrode to functional layer.

The maximum value of the dielectric permittivity obtained from the electrical field tunability measurements at 0 kV/cm applied field correlates well with the dielectric permittivity values after corrections (see Fig. 5). The results at high temperatures might be limited by increased conductivity. The same situation is also seen in Fig 3, where (low frequency) dielectric losses start to increase for temperatures around 480 K.

Figure 6a shows polarization-electric field (P-E) loops of the PMN-33PT thin film up to 150 kV/cm applied electric field. This PMN-33PT thin film shows a clear hysteresis property with a remnant polarization of $2P_r \approx 10\ \mu C/cm^2$ and a coercive field of $2E_c \approx 12$ kV/cm in the temperature range 300 – 380 K (see Fig. 6b). These results correspond well with the results presented by K. Wasa et al. [10]. The shape of the hysteresis loop of PMN-33PT thin film is sloped and slim. PMN-PT is a typical relaxor ferroelectric material which has nanodomain structure [14–16]. The nanodomains of the relaxor can be oriented with the field leading to large polarization. However, most of these domains re-acquire their random

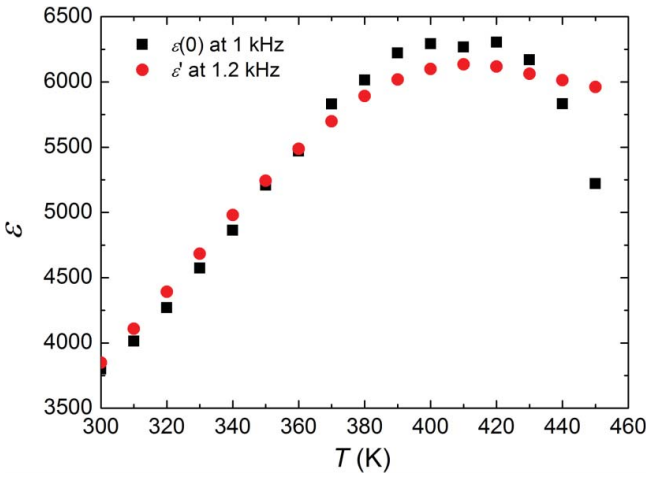

Figure 5. Temperature dependence of the dielectric permittivity obtained from Johnson approximation in the Landau-Ginsburg-Devonshire theory (black squares) and from dielectric permittivity results after electrode resistivity correction (red squares).

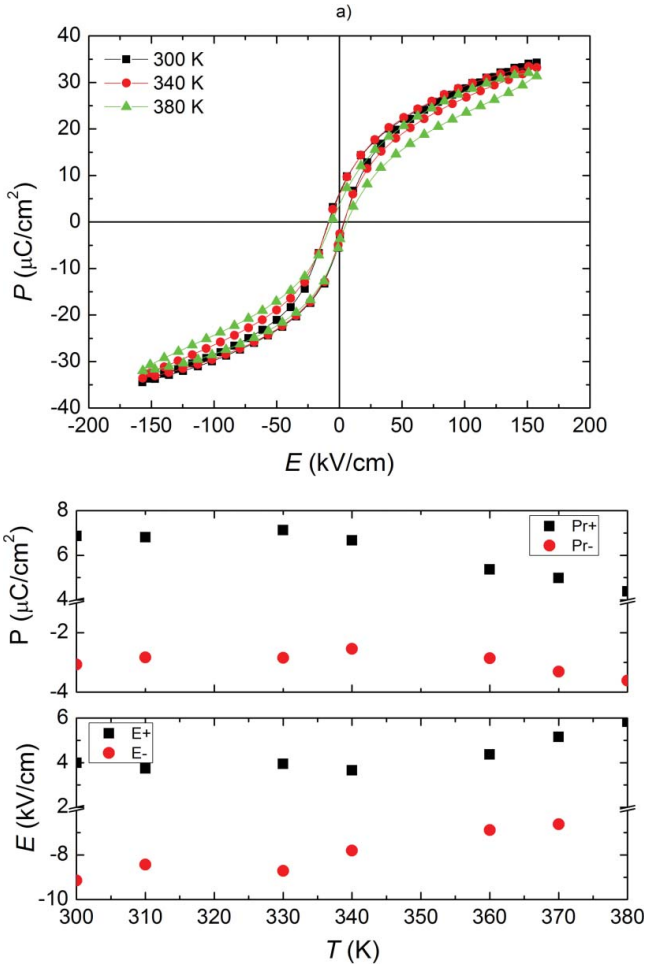

Figure 6. (a) Ferroelectric hysteresis curves of PMN-33PT thin film at different temperatures. (b) Temperature dependence of remnant positive and negative (Pr+ and Pr- respectively) polarization and positive and negative coercive field (E+ and E- respectively).

orientation resulting in a small remnant polarization when the applied electric field is removed [17–18].

Conclusions

This paper presents a systematic investigation into the electric properties of a PMN-33PT epitaxial thin film as function of temperature and frequency. Electric field tunability of the real part of dielectric permittivity is well approximated by the Johnson relation of the Landau-Ginsburg-Devonshire theory. It was observed that the position of the maximum of the dielectric permittivity depends on the direction of the change in the applied electric field. This might be due to charge injection from bottom electrode to functional layer. Also P-E loops up to 150 kV/cm applied electric field were measured. The PMN-33PT thin film shows a slight hysteresis with a remnant

polarization of $2P_r \approx 10\ \mu C/cm^2$ and a coercive field $2E_c \approx 12$ kV/cm in the temperature range 300 – 380 K.

Funding

This work has been financed by the Lithuanian-Swiss cooperation programme "Research and development" joint research project "SLIFE," project code LSP-12 007.

References

1. M. D. Nguyen, H. N. Vu, D. H. A. Blank, G. Rijnders, *Adv. Nat. Sci.: Nanosci. Nanotechnol.* **2**, 015005 (2011).
2. D. Isarakorn, A. Sambri, P. Janphuang, D. Briand, S. Gariglio, J.-M. Triscone, F. Guy, J. W. Reiner, C. H. Ahn, N. F. de Rooij, *J. Micromech. Microeng.* **20**, 055008 (2010).
3. M. Sepliarsky, RE Cohen, First-principles based atomistic modeling of phase stability in PMN-xPT. *J. Phys.: Condens. Matter.* **23**, 435902 (2011).
4. H. Fu, R. E. Cohen, Polarization rotation mechanism for ultrahigh electromechanical response in single-crystal piezoelectrics. *Nature.* **403**, 281–283 (2000).
5. S. E. Park, T. R. Shrout, *IEEE Trans. Ultrason. Ferroelectr. Freq. Control* **44**, 1140 (1997).
6. Seung-Hyub Baek, Mark S. Rzchowski, A. Vladimir, Aksyuk. Giant piezoelectricity in PMN-PT thin fi lms: Beyond PZT.
7. M. Davis, D. Damjanovic, N. Setter, Pyroelectric properties of $(1-x)Pb(Mg_{1/3}Nb_{2/3})O_3$-$xPbTiO_3$ and $(1-x)Pb(Zn_{1/3}Nb_{2/3})O_3$-$xPbTiO_3$ single crystals measured using a dynamic method. *J. Appl. Phys.* **96**(5), 1 September 2004.
8. K. Wasa, I. Kanno, T. Suzuki, S. H. Seo, D. Y. Noh, H. Okino, T. Yamamoto, Structure and Ferroelectric Properties of Sputtered PMNT Thin Films. 2004 IEEE International Ultrasonics, Ferroelectrics, 12 and Frequency Control Joint 50th Anniversary Conference..
9. K. Wasa, S. H. Seo, D. Y. Noh, I. Kanno, T. Suzuki, Heteroepitaxial growth of stress free single crystal perovskite thin films. *Surface Review and Letters* **13**(2 & 3), 167–172 (2006).
10. K. Wasa, I. Kanno, T. Suzuki, Structure and Electromechanical Properties of Quenched PMN-PT Single Crystal Thin Films. *Advances in Science and Technology* **45**, 1212–1217 (2006).
11. M. Boota, E. P. Houwman, M. Dekkers, M. Nguyen, G. Rijnders, Epitaxial $Pb(Mg_{1/3}Nb_{2/3})O_3$-$PbTiO_3$ (67/33) thin films with large tunable self-bias field controlled by a $PbZr_{1-x}Ti_xO_3$ interfacial layer. *Appl. Phys. Lett.* **104**, 182909 (2014).
12. M. D. Nguyen, H. Nazeer, K. Karakaya, S. V. Pham, R. Steenwelle, M. Dekkers, L. Abelmann, D. H. A. Blank, G. Rijnders, *J. Micromech. Microeng.* **20**, 085022 (2010).
13. C. Ang, Z. Yu, dc electric-field dependence of the dielectric constant in polar dielectrics: Multipolarization mechanism model. *Phys. Rev. B* **69**, 174109 (2004).
14. H. Idink, B. White W, Raman-spectroscopic study of order-disorder in lead magnesium niobate. *J. Appl. Phys.* **76**(3), 1789–1793 (1994).
15. W. Qu, X. Zhao, X. Tan, Evolution of nanodomains during the electric-field-induced relaxor to normal ferroelectric phase transition in a Sc-doped $Pb(Mg_{1/3}Nb_{2/3})O_3$ ceramic. *J. Appl. Phys.* **102** (8), 084101–1–8 (2007).
16. F. Jiang, S. Kojima, Study of three different relaxor ferroelectrics by high resolution micro-Brillouin scattering. *Jpn. J. Appl. Phys.* **39**(9B), 5704–5710 (2000).
17. G. A. Samara, The relaxational properties of compositionally disordered ABO_3 perovskites. *J. Phys.: Condens. Matter* **15**(9), R367–R411 (2003).
18. S. B. Vakhrushev, A. A. Naberezhnov, B. Dkhil, et al. Structure of Nanodomains in Relaxors. *Fundamental Physics of Ferroelectrics* **677**, 74–83 (2003).